



SYNTHESIS AND CHARACTERISATION OF NANOCRYSTALLINE CERIA POWDER (CeO₂) BY MICROWAVE INDUCED COMBUSTION METHOD

**P. SURIKALA^{*}, K. TAMILARASAN^a and
M. KANAGASABAPATHY^b**

Department of Physics, Rajapalayam Rajus, College, RAJAPALAYAM (T.N.) INDIA

^aDepartment of Physics, Kongu Engineering College, ERODE (T.N.) INDIA

^bDepartment of Chemistry, Rajapalayam Rajus, College, RAJAPALAYAM (T.N.) INDIA

ABSTRACT

Nanocrystalline Ceria powder was profitably synthesized by microwave induced combustion route using different composition of cerium nitrate as a precursor and glycine and sorbitol as a fuel. The powders were investigated by XRD, SEM, TEM, UV-visible and FTIR spectroscopy measurements. In our experiment, our sample CeO₂ powders showed that the average crystallite size ranged from 25 to 4 nm and lattice parameter ranged from 5.4218 to 5.4615 Å and also compared with Williamson-Hall plot and Nelson-Riley plot, respectively. This variation in size and lattice parameter was due to preparation conditions such as fuel ratio and rate of reaction and also structural distortion. There is an increase in micro strain calculated from Stoke's and Wilson formula with the small crystallite size. The structural morphology was analyzed by SEM and TEM. FTIR spectrum was purely matched with XRD spectrum. The optical band gaps of the powders were observed in the range of 3.04 to 2.58 eV. Lattice contraction with decreasing particle size, strongly indicating surface tension plays a major role.

Key words: Ceria, Microwave synthesis, XRD, SEM, TEM, FTIR, UV-Vis.

INTRODUCTION

Energy shortage and environment pollutions (CO₂ levels in the atmosphere touched 400 parts per million on May 9, 2013) are too crucial challenges the world facing today. Nanocrystalline materials could help in developing new energy sources and treat the pollutions. Ceria (CeO₂) is one of the most important remunerative rare earth oxide materials, widely used in the field of energy-environment¹, ultraviolet blocking materials²,

^{*} Author for correspondence; E-mail: psuriakala@gmail.com

oxygen gas sensors³ and spintronics⁴, etc. Nanostructure ceria materials with diverse properties could help in developing new energy sources of solid oxide fuel cells⁵ and treat the pollutions in three way catalysts⁶. Cerium oxide is also well known for its optical properties and it can filter ultraviolet (UV) rays up to 370 nm. Cerium oxide is a semi-conducting material with a band gap of around 3.0-3.2 eV. Ultrafine ceria has been used as a sun screen material for its excellent ultraviolet absorption property⁷. Ceria has shown ferromagnetic behavior due to its oxygen deficiency⁸.

By considering the importance of nanocrystalline ceria for different applications, various synthesis methods were adopted viz, co-precipitation⁹, micro emulsion¹⁰, high energy ball milling and liquid processing¹¹, sono chemical and microwave techniques¹². When compared to other techniques for the synthesis of nanocrystalline ceria powder, microwave induced combustion method is a simple and better one, low in cost, time saving and low energy consumption. In our study, glycine and sorbitol were used as fuels for the synthesis and characterization of nano crysatalline ceria powder using cerium nitrate for various industrial applications.

EXPERIMENTAL

All the reagents used for the preparation were analytically pure. Here, cerium nitrate $\text{Ce}(\text{NO}_3)_3 \cdot 6\text{H}_2\text{O}$ acts as precursor material for CeO_2 and glycine and sorbitol acts as fuels. For stock solution preparations, de-ionized water was used. For the preparation of CeO_2 , stock solution of cerium nitrate with various concentrations (0.25 mol, 0.5 mol and 0.75 mol) were prepared and stored at room temperature. 100 mL of the 0.25 mol of $\text{Ce}(\text{NO}_3)_3 \cdot 6\text{H}_2\text{O}$ were well mixed with 2 mL of glycine and 2 mL of sorbitol. The fuel concentration was fixed and the cerium nitrate concentration was varied as per the stock solution prepared. Then, the beaker was introduced into the microwave oven (Samsung 900W & 2450 HZ), conventionally heated at 250°C for 10 min and then applied a microwave power at 300 W for 10 min. A lot of fumes were observed during the microwave heating reaction. Finally a light yellow in color powder product was obtained and named as (CEA). The same experimental procedures were followed for other two molar concentrations; the final products were named as CEB (0.5 mol) and CEC (0.75 mol). Details of experimental process were shown in Table 1.

The X-ray diffraction (XRD) patterns of the powder samples were measured at room temperature with Bruker Axs D8 Advance diffractometer with $\text{CuK}\alpha$ radiation of wavelength 1.5418 Å. Molecular structure and bonding characteristics was analyzed using FTIR (Thermo Nicolet, Avatar 370). Optical properties of nano-crystalline ceria were

studied by UV-Vis – NIR Spectrophotometer (Varian, Cary 5000). The microstructure morphology and the elemental composition of the prepared powders was analyzed by Scanning Electron Microscopy (JEOL Model JSM-6390LV), and Transmission Electron Microscopy (JEOL JEM 2100).

Table 1: Preparation details of pure ceria sample

S. No.	Stock solution		Chemical composition (Mixture) taken for synthesis	Characteristic of microwave oven used	Final product name
	Starting material	Fuel			
1	10.85 g of Ce(NO ₃) ₃ .6H ₂ O mixed with 100 mL of water				CEA
2	21.7 g of Ce(NO ₃) ₃ .6H ₂ O mixed with 100 mL of water	3.75 g of Glycine dissolved into 100 mL of water	100 mL of Cerium Nitrate + 2 mL of Glycine + 2 mL of Sorbitol	250°C 10 min and 300 W 10 min	CEB
3	32.5 g of Ce(NO ₃) ₃ .6H ₂ O mixed with 100 mL of water				CEC

RESULTS AND DISCUSSION

X-Ray diffraction

Ceria exhibit a face centered cubic crystal structure of fluorite type (Space group: Fm-3 m), in which Ce ions are cubic close packed and O ions are in the tetrahedral space. Fig. 1 shows the powder XRD pattern of ceria powder using various stock solution of cerium nitrate and fuel ratio. The peaks were indexed as per the JCPDF #34-0394. It clearly shows that except the ceria peaks, there is no additional peak. It reveals that the material is in phase pure ceria and also indicates that the powder is random crystallites without any orientation. The ceria powders prepared in the lower concentration of cerium nitrate (0.25 mol) shows a good crystalline material and narrow peaks with an average crystallite size of about 25 nm whereas the powders from the higher concentration of nitrate/fuel ratio indicates that there is a very broad peaks with crystallite size of 7 nm and 4 nm for 0.5 mol and 0.75 mol, respectively. The variation in the sizes of the crystallite was due to concentration of cerium nitrate, amount of fuel in use for preparation and microwave power. Preparation method can be kept constant amount of fuel and microwave powder for all the samples. So the lower concentration of the cerium nitrate with fuel ratio can have faster rate of reaction and higher reaction temperature result increase of crystallite size. Milder reaction obtained in higher concentration of cerium nitrate result decrease of crystallite size. The

value of the crystallite size was compared with Williamson-Hall plot shown in Fig. 2, which was agreed with the crystallite size calculated from Scherrer formula.

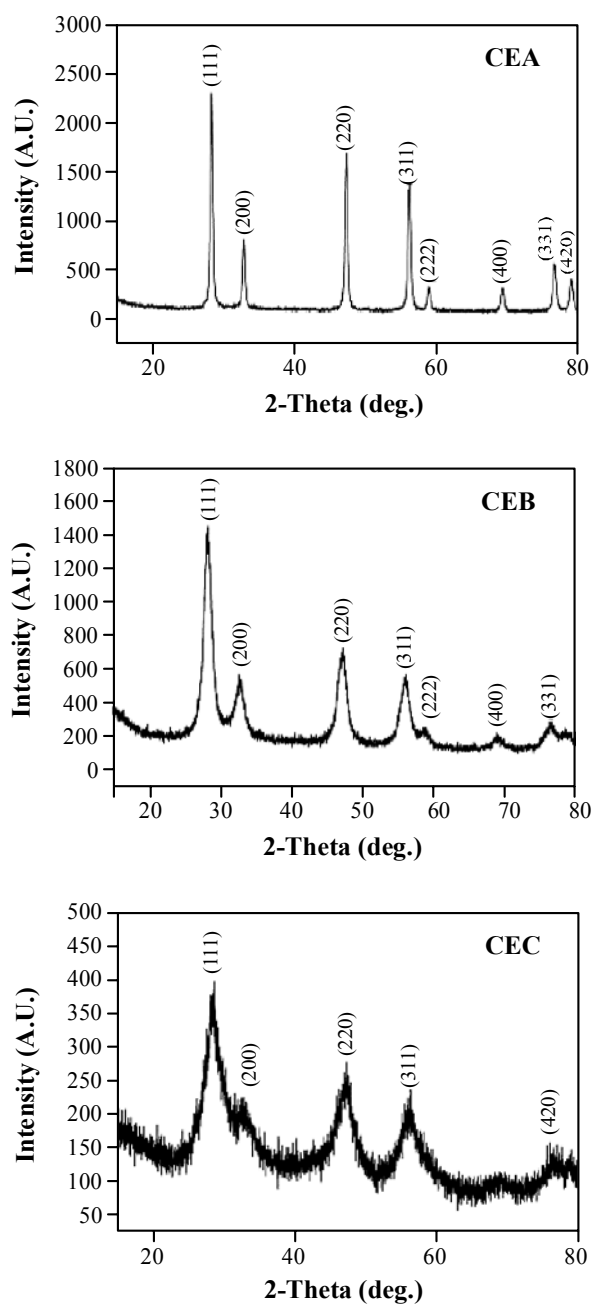


Fig. 1: XRD pattern ceria powder

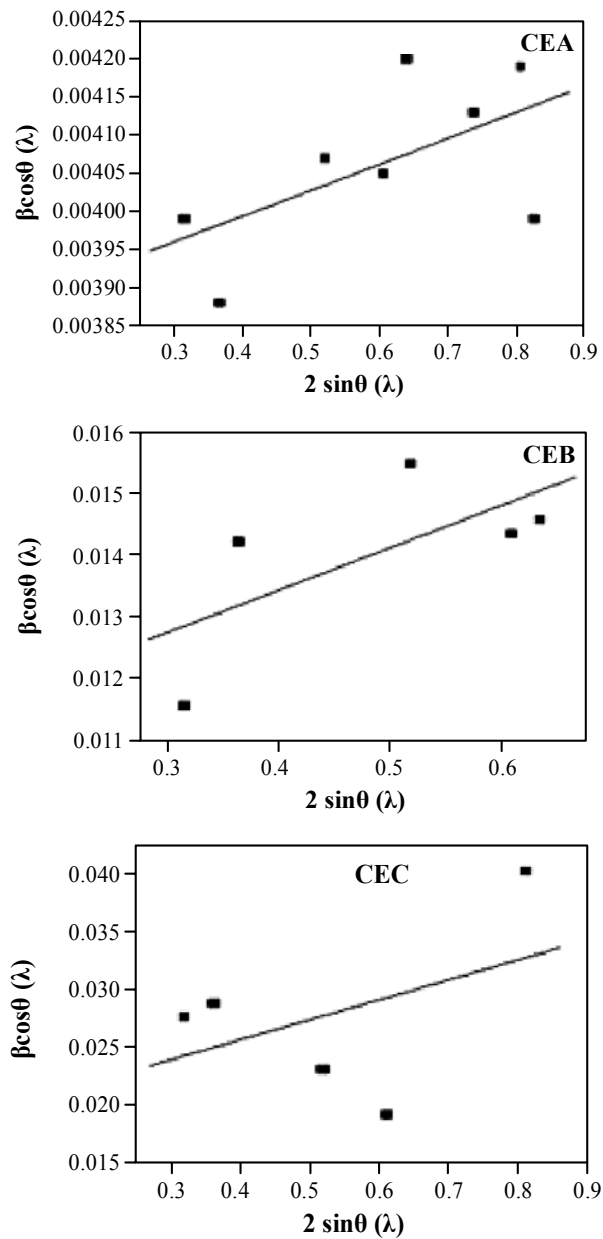


Fig. 2: Williamson–Hall plot of ceria powder

In order to study the structural parameters of these powders, the lattice parameter were calculated from their two theta values as per the standard procedure for cubic system. The lattice parameters obtained from our experiment are in agreement with data reported in literature¹³ ($a = 5.411 \text{ \AA}$) with small amount of difference. The variation in lattice parameter

caused by the forces exerted between grains during synthesis, are seen to decrease by around an order of magnitude after initial heat treatment. The extraction of accurate two theta from these nano crystalline material is little difficult. To get accurate lattice parameters, the Rietveld method of analysis using Powdercell code¹⁴ and Nelson-Riley plot is (Fig. 3) were used. The resulting final Rietveld plots of all the samples are shown in Fig. 4.

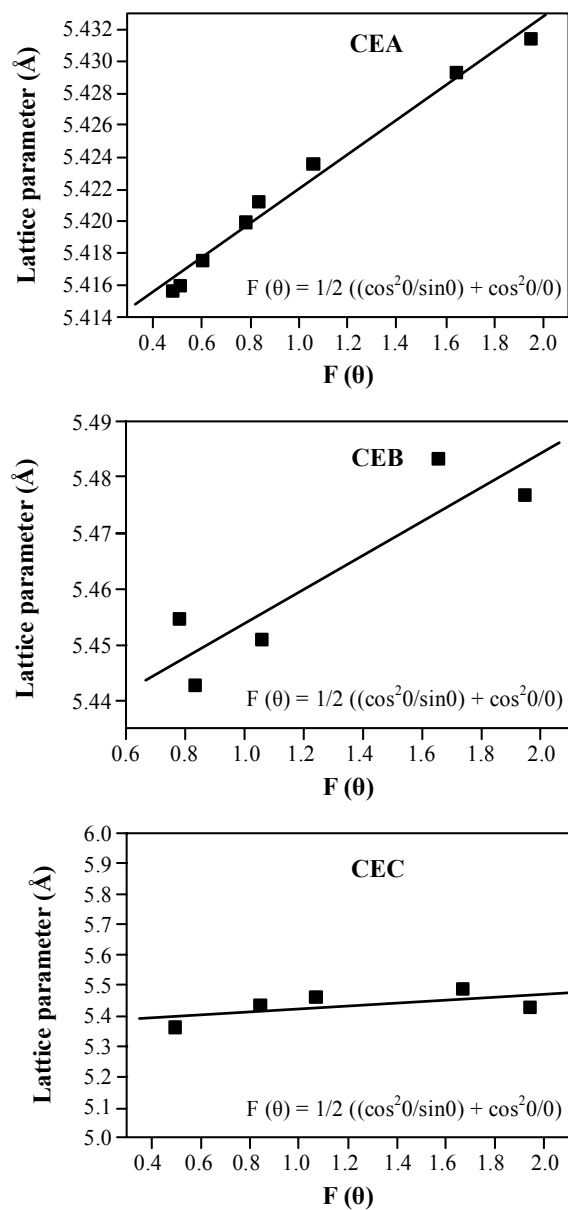


Fig. 3: Nelson-Riley plot of ceria powder

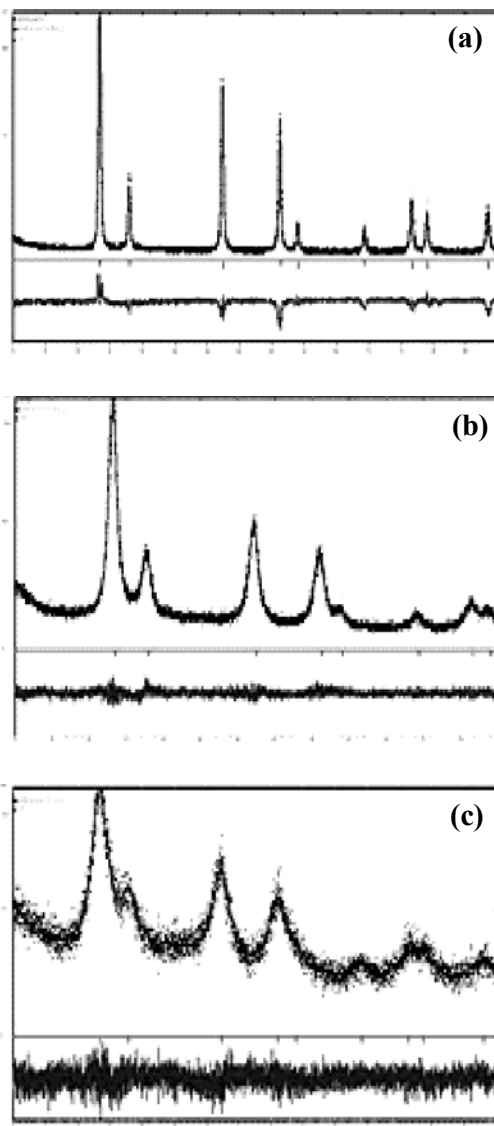


Fig. 4: Typical Rietveld final plot of CeO_2 powders prepared from various nitrate/fuel ratio (a) CEA (b) CEB and (c) CEC

The micro structural parameters such as micro strain of powders are determined from their broadening using standard procedures of Williamson-Hall relation adopted in the Rietveld code itself.

The results were recorded in Table 2. It was observed that when the cerium nitrate concentration increases, there was a decrease in the crystallite size and increase of micro

strain in the lattice. The powder prepared from the lowest cerium nitrate concentration, the lattice parameter was very close to the standard ceria lattice parameter. The powder prepared using the higher cerium nitrate concentration was found to be higher lattice parameter value. This may be also influence the small crystallite size, large lattice strain and the conditions adopted for preparation.

Table 2: Structural and micro structural parameters of the ceria powders

Sample	Crystallite size (nm)		Lattice parameter (Å)		Strain	
	Scherrer method	Williamson-Hall	Bragg's formula	Nelson-Riley Plot	Convention method	Williamson Hall
CEA	25.4	25.9	5.4218	5.41126	3.5×10^{-3}	7.010×10^{-4}
CEB	6.8	7.9	5.4615	5.42352	1.3×10^{-2}	0.01381
CEC	3.5	4.4	5.4318	5.39457	3.2×10^{-2}	0.03503

Morphology and microstructure by TEM and SEM

Fig. 5 gives the TEM image of the powder obtained for the composition of 0.75 mol of $\text{Ce}(\text{NO}_3)_3 \cdot 6\text{H}_2\text{O}$. The selected Area Electron Diffraction (SAED) image of the CEC powder clearly shows the ring pattern indicating the powder was polycrystalline nature and confirms the presence of CeO_2 . SEM images of the various powders prepared at various concentrations of cerium nitrates and fuel are shown in Fig. 6. From this figure, it was observed that at the lower concentration of cerium nitrate shows crystalline grains, whereas the powders prepared at higher nitrate concentration shows the large size foamy agglomerates with voids having wide distribution of sizes. This is due to sudden release of a large amount of gas during the combustion synthesis^{15,16}. It confirms that, the cerium nitrate and fuel ratio was one of the important parameters to get the nanocrystalline ceria powders.

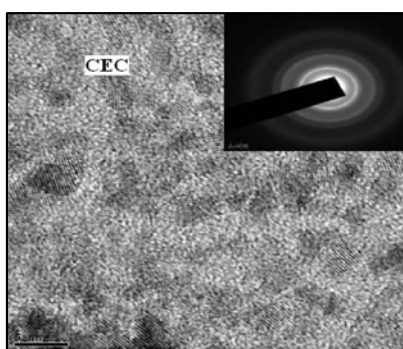


Fig. 5: TEM image and SAED

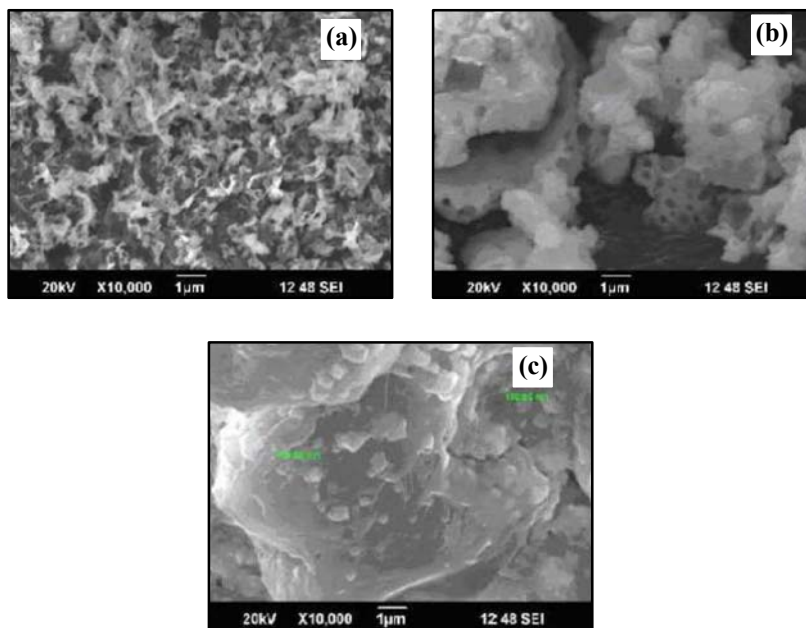


Fig. 6: SEM images

FTIR

The FT-IR spectra of the as-prepared CeO₂ samples are shown in Fig. 7. The band below 500 cm⁻¹ is attributed to Ce–O stretching band and it confirms the formation of CeO₂ for all samples. Ceria has the ability to absorb water molecules from the surrounding environment; thus, the peak at 3400 cm⁻¹ corresponds to the physically adsorbed water on the samples. The sharp peak at about 1600 cm⁻¹ is assigned to C–O stretching band of the adsorbed CO₂ of air on the surface of ceria nano powders. Residual water and a hydroxyl group are usually detected in the as-prepared ceria samples regardless of synthesis method used and further heat treatment is necessary for their elimination. The band around in Finger print zone may be 1384 cm⁻¹ is due to sp C-H bending mode of vibration. The band around 1045 cm⁻¹ is due to C-O alkoxy bond. These two bands indicate excess of fuel was present. Excess of fuel was present only in the sample prepared from higher concentration of cerium nitrate. The FTIR spectrum of the as-prepared ceria also exhibits strong broad band below 700 cm⁻¹, which is due to the envelope of the phonon band of the metal oxide network. Lower concentration of cerium nitrate was utilized all the amount of fuel thereby increasing the rate of reaction and reaction temperature and higher concentration of cerium nitrate taken only sufficient amount of fuel, so that milder reaction was carried out during preparation. FTIR spectrum was fully agreed with X-Ray diffraction spectrum.

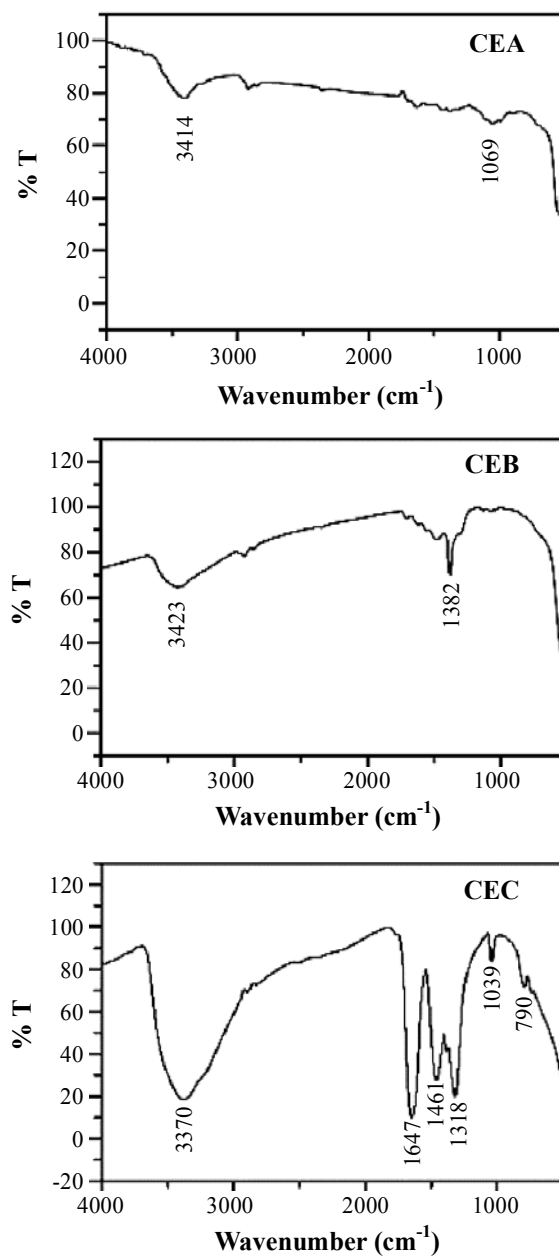


Fig. 7: FTIR spectrum

UV-Vis Spectrum

The UV-visible absorption spectra of the CeO₂ samples are shown in Fig. 8. All the samples showed a strong absorption below 500 nm. The samples CEA and CEB have shown

the absorbance edge around 458 nm and 409 nm whereas the absorption edge of CEC was around 482 nm. The band gap of the powders was determined by the equation h^*C/λ from the cut off wavelength^{17,18} (Table 3). It can be seen that there was a very sharp absorption edge from the lower concentration of cerium nitrate route whereas the powder from the higher concentration of cerium nitrate/fuel ratio shows, a blunt absorption edge. This characteristic behavior may be due to the excess of fuel of carbon impurities¹⁹ present in the powders during the synthesis which was confirmed in FTIR.

Table 3: Optical band gap values of ceria powder

Sample	λ (m)	E (J)	Optical band gap (eV)
CEA	4.58E-07	4.35E-19	2.72
CEB	4.09E-07	4.86E-19	3.04
CEC	4.82E-07	4.13E-19	2.58

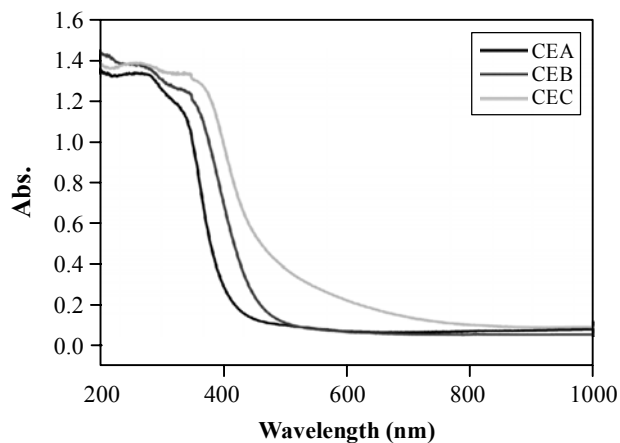


Fig. 8: UV-Vis spectrum

CONCLUSION

Nanocrystalline CeO₂ powder was successfully synthesized by microwave assisted combustion method using various nitrate/fuel ratios. XRD studies showed that there was a phase pure ceria and the average crystallite size of the CeO₂ nanoparticles found in ranges from 25 nm to 4 nm at various nitrate/fuel ratios. It was observed that the sizes of the nanocrystallite decreases with the increase of cerium nitrate concentration. This lattice parameter variation of prepared powders with respect to standard CeO₂ lattice is due to preparation conditions. The different particle morphology of the ceria powders was observed

with variation of the initial cerium nitrate composition by SEM studies. The band gap values were measured from the absorption edges from UV-Vis absorption spectra and found good agreement with the literature values.

REFERENCE

1. C. Sun, H. Li and L. Chen, *Energy Environ. Sci.*, **5**, 8475 (2012).
2. Zholobak, V. K. Ivanov, A. B. Shcherbakov, A. S. Shaporev, O. S. Polezhaeva and A. Y. Baranchikov, *J. Photoch. Photobio. B*, **102**, 32 (2012).
3. P. Jasinski, T. Suzuki and H. U. Anderson, *Sensors and Actuators B*, **95**, 73 (2003).
4. P. K. Slusser, *Transition Metal Doped Cerium Oxide for Spintronics Applications*, A, Thesis Submitted to Department of Materials Science and Engineering University of Utah (2009).
5. Z. Liu, D. Ding, M. Liu, X. Ding, D. Chen, X. Li, C. Xia and M. Liu, *J. Power Sources* (2013).
6. G. Kim, *Ind. Eng. Chem. Prod. Res. Dev.*, **21**, 267 (1982).
7. S. Yabe, M. Yamashita, S. Momose, K. Tahira, S. Yoshida, R. Li, S. Yin and T. Sato, *Int. J. Inorg. Mater.*, **3**, 1003 (2001).
8. Q. Y. Wen, H. W. Zhang, Y. Q. Song, Q. H. Yang, H. Zhu and J. Q. J. Xiao, *Phys. Condens. Matter.*, **19**, 246205 (2007).
9. P. Nachimuthu, W.-C. Shih, R.-S. Liu, L.-Y. Jang and J.-M. Chen, *J. Solid State Chem.*, **149**, 408 (2000).
10. S. Gupta, P. Brouwer, S. Bandyopadhyay, S. Pati, R. Briggs, J. Jain and S. Seal, *J. Nanosci. Nanotechnol.*, **5**, 1101 (2005).
11. A. Sharma, S. Bhattacharya, S. Das and K. Das, *Int. Conference on Nanotechnol. Biosensors* (2010).
12. E. Kumar, P. Selvarajan, K. Balsubramanian, *Recent Res. Sci. Technol.*, **2**, 37 (2010).
13. M. Wolczyk and L. Kepinski, *J. Solid State Chem.*, **99**, 409 (1992).
14. T. J. B. Holland and S. A. T. Redfern, *Mineralogical Magazine*, **61**, 65 (1997).
15. E. Esmaeili, A. Khodadadi and Y. Mortazavi, *J. Eur. Ceram. Soc.* (2008).
16. R. V. Mangalaraja, S. Ananthakumar, Kasimayan Uma, Romel, M. Jimenez, Marta Lopez and Carlos P. Camurri, *Mater. Sci. Engg. A*, **517**, 91 (2009).

17. M. Hoffman, S. Martin, W. Choi and D. Bahnemann, *Chem. Rev.*, **95**, 69 (1995).
18. J. Wade, An Investigation of TiO₂-ZnFe₂O₄ Nanocomposites for Visible Light Photo Catalysis, A Thesis Submitted to Department of Electrical Engineering, College of Engineering, University of South Florida (2005).
19. A. Zaleska, *Recent Patents on Engineering*, **2**, 157 (2008).

Revised : 04.05.2015

Accepted : 06.05.2015